Ambipolar organic field-effect transistors based on a solution-processed methanofullerene

Anthopoulos, Thomas D.; Tanase, Cristina; Setayesh, Sepas; Meijer, Eduard J.; Hummelen, Jan C.; Blom, Paul W.M.; de Leeuw, Dagobert

Published in:
Advanced materials

DOI:
10.1002/adma.200400309

Publication date:
2004

ADVANCED MATERIALS

for design considerations of passive matrix displays based on organic light-emitting devices (LEDs), where short current bursts are used to drive individual pixels to very high brightnesses. Our observations demonstrate that cooling of organic films can occur very rapidly with rates of up to 10 mK ns^{-1}, suggesting that heat build-up in displays driven under pulsed operation can be minimized. Finally, we note that the externally triggered fluorescence burst in effect provides a direct visualization of the three level system intrinsic to organic molecules. Intermolecular depopulation of the meta-stable triplet state by radiative singlet emission can be tapped externally by allowing gated energy transfer from the hot band to, for example, a fluorescent host, whose singlet lifetime is much shorter than the PtOEP triplet. This could enable excitation of a material without optically or electrically injected charge carriers. Long-lived meta-stable states, which can be depopulated by thermally assisted radiative transitions, have recently been made responsible for the surprisingly large device efficiencies observed in bulk heterojunction LEDs.[26] The depopulation of the PtOEP triplet is conceptually similar to this, although it occurs on an intramolecular level, and may provide helpful insight into understanding spin statistics in organic LEDs.

Experimental

PtOEP was dispersed in polystyrene at a concentration of 11 wt.-% and dissolved in toluene. Heating strip lines of typical dimensions 8×2 mm were made by depositing a thin layer of gold (typically 100 nm) on top of a glass substrate. The strips were terminated by large area contact pads. The polymer films were spin-coated onto the substrates and mounted in a cryostat under vacuum. Optical excitation was achieved using a nitrogen pumped dye laser at 387 nm, tuned to the narrow Sorret absorption band of PtOEP [20]. The laser spot was focused to a spot diameter of approx. 500 μm. The samples could be heated on the microsecond time scale using a high power pulse generator with a peak power of 1.8 kW. PL spectra were recorded using a Princeton Instruments gated intensifier coupled to a cooled charge-coupled device (CCD) and a 0.25 m monochromator with typical integration times of 20 s (i.e., 400 laser pulses). Time integrated photoluminescence was measured by increasing the gate length to 900 μs, i.e., much longer than the excited state lifetime. This was found to be equivalent to time integrated detection using a standard, non-gated detector.

Received: February 27, 2004
Final version: June 7, 2004

[1] J. L. Clark, G. Rumbles, *Phys. Rev. Lett.* **1996**, *76*, 2037.
[2] J. M. Lupton, *Appl. Phys. Lett.* **2002**, *80*, 186.
[3] B. A. Hooper, Y. Domankevitz, R. R. Anderson, C. Lin, *Appl. Phys. Lett.* **2001**, *78*, 2381.
[4] J. Lou, M. Finegan, P. Mohsen, T. A. Hatton, P. A. Laibinis, *Rev. Anal. Chem.* **1999**, *18*, 235.
[5] S. W. Allison, G. T. Gillies, *Rev. Sci. Instrum.* **1997**, *68*, 2615.
[6] M. Engeser, L. Fabbrizzi, M. Licchelli, D. A. Sacchi, *Chem. Commun.* **1999**, *13*, 1191.
[7] R. E. Brewster, M. J. Kidd, M. D. Schuh, *Chem. Commun.* **2001**, *12*, 1134.
[8] S. F. Collins, G. W. Baxter, S. A. Wade, T. Sun, K. T. V. Grattan, Z. Y. Zhang, and A. W. Palmer *J. Appl. Phys.* **1998**, 84, 4649.
[9] K. T. V. Grattan, A. W. Palmer, Z. Zhang, *Rev. Sci. Instrum.* **1991**, *62*, 1210.
[10] R. R. Sholes, J. G. Small, *Rev. Sci. Instrum.* **1980**, *51*, 882.
[11] S. A. Wade, S. F. Collins, G. W. Baxter, *J. Appl. Phys.* **2003**, *94*, 4743.
[12] S. F. Collins, G. W. Baxter, S. A. Wade, T. Sun, K. T. V. Grattan, Z. Y. Zhang, A. W. Palmer, *J. Appl. Phys.* **1998**, *84*, 4649.
[13] N. Tessler, N. T. Harrison, D. S. Thomas, R. H. Friend, *Appl. Phys. Lett.* **1998**, *73*, 732.
[14] C. R. Smith, D. R. Sabatino, R. J. Praisner, *Exp. Fluids* **2001**, *30*, 190.
[15] S. Chen, I.-Y. S. Lee, W. A. Tolbert, X. Wen, D. D. Dlott, *J. Phys. Chem.* **1992**, *96*, 7178.
[16] A. Seilmeier, P. O. J. Scherer, W. Kaiser, *Chem. Phys. Lett.* **1984**, *105*, 140.
[17] D. G. Cahill, K. Goodson, A. Majumdar, *J. Heat Transfer* **2002**, *124*, 223
[18] F. A. Boroumand, A. Hammiche, G. Hill, D. G. Lidzey, *Adv. Mater.* **2004**, *16*, 252
[19] J. M. Lupton, *Appl. Phys. Lett.* **2002**, *81*, 2478.
[20] J. M. Lupton, J. Klein, *Chem. Phys. Lett.* **2002**, *363*, 204.
[21] M. A. Baldo, D. F. Obrien, Y. You, A. Shoustikov, S. Sibley, M. E. Thompson, S. R. Forrest, *Nature* **1998**, *395*, 151.
[22] V. Cleave, G. Yahioglu, P. Le Barny, R. H. Friend, N. Tessler, *Adv. Mater.* **1999**, *11*, 285.
[23] G. Ponterini, N. Serpone, M. A. Bergkamp, T. L. Netzel, *J. Am. Chem. Soc.* **1983**, *105*, 4639.
[24] A. Gilbert, J. Baggott, in *Essentials of Molecular Photochemistry*, Blackwell Scientific Publishers, Oxford , UK **1995**, p. 107.
[25] J. B. Callis, M. Gouterman, Y. M. Jones, B. H. Henderson, *J. Mol. Spectrosc.* **1971**, *39*, 410.
[26] A. C. Morteani, A. S. Dhoot, J.-S. Kim, C. Silva, N. C. Greenham, C. Murphy, E. Moons, S. Ciná, J. H. Burroughes, R. H. Friend, *Adv. Mater.* **2003**, *15*, 1708.

Ambipolar Organic Field-Effect Transistors Based on a Solution-Processed Methanofullerene**

By *Thomas D. Anthopoulos*,* *Cristina Tanase*, *Sepas Setayesh*, *Eduard J. Meijer*, *Jan C. Hummelen*, *Paul W. M. Blom*, and *Dago M. de Leeuw*

In recent years, there has been ample demonstration of electronic devices employing organic semiconducting materials as the electroactive elements.[1–5] Organic semiconductors are attractive because they offer the prospect for large-area,

[*] Dr. T. D. Anthopoulos, Dr. S. Setayesh, Dr. E. J. Meijer, Dr. D. M. de Leeuw
Philips Research Laboratories
Prof. Holstlaan 4 (WAG), NL-5656 AA Eindhoven (The Netherlands)
E-mail: thomas.anthopoulos@philips.com
C. Tanase, Prof. J. C. Hummelen, Prof. P. W. M. Blom
Molecular Electronics, Materials Science Centre Plus
University of Groningen
Nijenborgh 4, NL-9747 AG Groningen (The Netherlands)

[**] T. D. Anthopoulos gratefully acknowledges financial support from the EC under project No: HPRN-CT-2002-00327 (EUROFET). The work of C. Tanase forms part of the research program of the Dutch Polymer Institute project No. 276.

  DOI: 10.1002/adma.200400309

low-cost, and flexible-device applications.[6,7] One of the most important electronic devices is the transistor since it represents the building block of analog as well as digital-circuit architectures. During the past twenty years, there have been numerous reports on transistors employing small molecules, polymers, and other organic semiconductors.[3,8] A distinct characteristic of nearly all these transistors is that they transport a single carrier type, either holes (p-type)[8–10] or electrons (n-type),[11–13] with the large majority being p-type. The simultaneous or selective transport of electrons and/or holes (the so-called ambipolar charge transport) in an organic transistor is a highly desirable property because it enables the design of circuits with low-power dissipation and good noise margins, similar to those encountered in complementary metal-oxide semiconductor (CMOS) logic circuits. Although the first single-channel inorganic ambipolar transistors have been demonstrated more than two decades ago,[14] their organic counterparts have only become a reality in recent years.[15–20] The first report on ambipolar operation in a single organic field-effect transistor (OFET) was for devices employing a p/n-type heterostructure as the active channel layer consisted of two carefully chosen organic semiconductors.[15,16] It was shown that currents of both polarities could be simultaneously injected from the source and the drain contacts under appropriate bias conditions, and both n- and p-type transistor operation could be achieved. More recently, ambipolar charge transport was reported for OFETs employing single films of heterogeneous blends consisting of polymer-based interpenetrating networks (first suggested by Tada et al.[17]), as well as for narrow-bandgap organic semiconductors.[19] Using these materials, the first complementary-like inverters employing single-channel OFETs have been demonstrated.[19] In their work, Meijer et al. argued that ambipolar transport is an intrinsic property of pure organic semiconductors, and that it is highly dependent on the energy-level matching between the work function of the source and drain electrodes with the energy levels, namely, the highest occupied molecular orbital (HOMO) and the lowest unoccupied molecular orbital (LUMO) of the semiconductor.[19]

Here, we report on OFETs based on the solution-processable methanofullerene [6,6]-phenyl-C_{61}-butyric acid methyl ester (PCBM) employing gold electrodes (Fig. 1a). In particular, we show for the first time that OFETs based on this molecule exhibit ambipolar-transport characteristics with the devices operating in hole- or electron-accumulation depending upon the biasing conditions. The present results qualify PCBM as a potential candidate for application in solution-processed complementary-like circuits, while at the same time providing further supporting evidence that ambipolar-charge transport is a generic property of pure organic semiconductors.

Figure 1a shows a schematic diagram of the top view and cross-section of the ring transistor studied using gold (Au) source and drain electrodes. We employed ring-type transistors in order to minimize contributions by parasitic currents.[21] A detailed description of the device fabrication

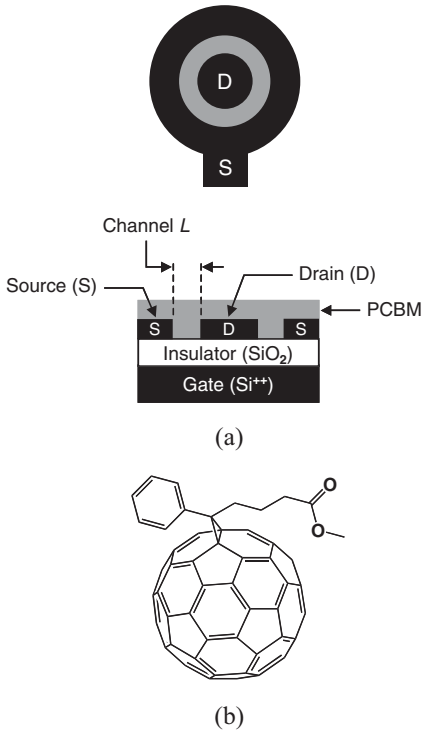

Figure 1. a) Schematic diagram of the top view and cross-section of the ring-type OFET geometry used in this study. The channel width (W) is equal to 1000 μm for all transistors studied, while the channel length (L) was varied within the range 0.75–40 μm. The drain and source electrodes consist of Au contacts. b) The molecular structure of PCBM.

process is given in the Experimental section. Figure 1b shows the molecular structure of PCBM. The n-channel transfer characteristics of a typical PCBM transistor ($W = 1000$ μm, $L = 20$ μm) measured at 293 K under high vacuum (10^{-5} Pa) are shown in Figure 2a. Prior to electrical characterization, all transistors were annealed at 393 K for several hours under high vacuum. The inset in Figure 2a shows the simplified energy-band diagram of PCBM[19] and Au electrodes in the absence of any bias potential or interface dipoles. When the gate is positively biased, a channel of accumulated electrons near the insulator/PCBM interface forms, and the electron current flowing through the channel is enhanced. This is evident in both $V_D = +2$ V and $V_D = +20$ V (V_D is the drain voltage) transfer characteristics shown in Figure 2a. Although one would expect the injection of electrons from gold into PCBM to be a difficult process (Fig. 2a, inset) due to the mismatch in the energies of the LUMO level of the PCBM and the work function of gold [$\phi_b(e^-) = 1.4$ eV], the transistor works at a low switch-on voltage ($V_{SO} < +3$ V) with the drain current $I_D \approx 10^{-6}$ A for an applied gate bias $V_G = +50$ V. The low value of V_{SO} is conventionally explained by the absence of any significant concentration of trap states in the channel. We note that by trap states we mean deep energy states introduced unintentionally in the form of chemical impurities, absorbed gas molecules, and/or structural defects. This observation is in accordance with the trap-free space-charge limited-current char-

ADVANCED MATERIALS

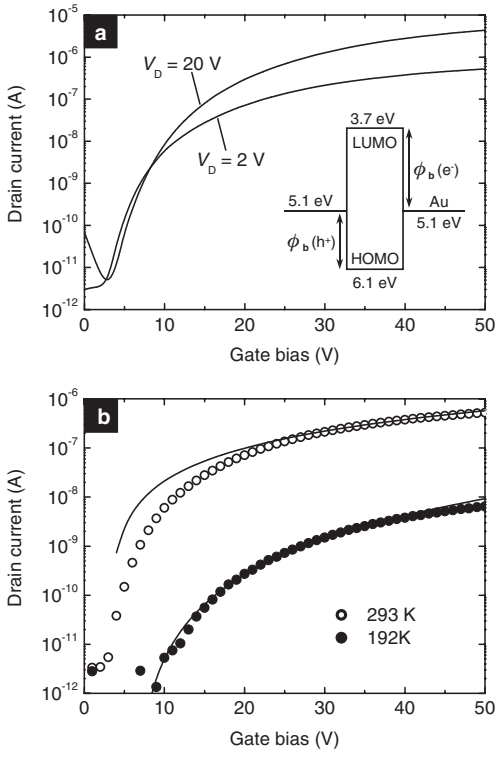

Figure 2. Transfer characteristics of a PCBM field-effect transistor (L = 20 μm) in n-channel operation. a) Transfer characteristics obtained at 293 K for V_D = +2 V and V_D = +20 V. Inset shows a simplified energy-band diagram of PCBM and Au (from ref. [19]) in the absence of any bias or interface-dipole layers. $\phi_b(h^+)$ and $\phi_b(e^-)$ are the injection barriers for holes and electrons, respectively. b) Transfer characteristics obtained at 192 K (●) and 293 K (○) with V_D = +2 V. Solid lines indicate the calculated drain currents using Equation 1.

acteristics observed in PCBM-based diodes.[22] It is worth noting that, in disordered semiconductors, even in the trap-free regime, carrier transport takes place via hopping between localized transport states due to the disorder in the material. In the presence of traps, however, the conductivity of the semiconductor is reduced, since a large fraction of the injected carriers will be trapped and consequently will not contribute to the conduction.

The relatively large value of I_D (~10^{-6} A) is also a good indication of the presence of a relatively small contact barrier at the PCBM/Au interface. This may be due to the formation of a strong interface dipole at the Au/PCBM interface, which lowers the barrier $\phi_b(e^-)$ by 0.64 eV, thus giving rise to an injection barrier of 0.76 eV.[23] A similar barrier reduction has been observed for the Au/C_{60} interface, as determined by UV photoemission spectroscopy.[24] The electron mobility (μ_e) in the linear regime was calculated from the transfer characteristics of Figure 2a for V_D = +2 V, yielding a maximum value of 9×10^{-3} $cm^2 V^{-1} s^{-1}$ at V_G = +30 V. The calculation for the saturation regime, where V_D = +20 V, yields a similar mobility of 1×10^{-2} $cm^2 V^{-1} s^{-1}$ at V_G = +20 V. In addition to the relatively high electron mobility, OFETs exhibit high ON–OFF current ratios (defined as the ratio of I_D at maximum V_G to I_D at $V_G = V_{SO}$) on the order of 10^6 with subthreshold slopes (S) of $S \sim 1$ V per decade. Although we use Au contacts, our measured electron mobility is more than a factor of two higher than electron mobilities reported previously for PCBM-based transistors employing calcium electrodes in a top-contact device configuration.[25] This difference is ascribed to the heat treatment of our samples for prolonged periods of time under high vacuum prior to characterization. Furthermore, the measured electron field-effect mobility exceeds the mobility obtained from SCLC measurements[22] by a factor of five due to the dependence of the mobility on charge-carrier density.[26] We note that all device characteristics were found to be strongly dependent on the annealing process and the ambient conditions following PCBM deposition. In this context, V_{SO} was found to decrease from +25 V to < +2 V after annealing, while the measured electron mobility increased by more than two orders of magnitude. It was also established that high vacuum, under which annealing is performed, was an essential processing condition in order to obtain the good performance characteristics of our OFETs. This drastic effect can likely be attributed to doping of the PCBM layer with ambient oxygen. The dopant sites act as electron traps that lead to a reduction in the number of mobile carriers and their mobility, and a subsequent increase in V_{SO}.

In order to obtain some insights into the electron-transport processes across the device, we fit the transfer characteristics using a disorder model of hopping, i.e., the thermally activated tunneling of carriers between localized transport states, in an exponential density of states[27] given as

$$I_D = \frac{WV_D \varepsilon_S \varepsilon_0 \sigma_0}{Le} \left(\frac{T}{2T_0 - T}\right) \times \sqrt{\frac{2k_B T_0}{\varepsilon_S \varepsilon_0}} \times \left[\left(\frac{T_0}{T}\right)^4 \sin\left(\pi \frac{T}{T_0}\right) \Big/ (2\alpha)^3 B_C\right]^{T_0/T} \times \left[\sqrt{\frac{\varepsilon_S \varepsilon_0}{2k_B T_0}} \left(\frac{C_i (V_G - V_{SO})}{\varepsilon_S \varepsilon_0}\right)\right]^{(2T_0/T-1)} \quad (1)$$

where W and L are the width and length of the channel respectively, e is the elementary charge, k_B is the Boltzmann constant, ε_S is the relative dielectric constant of the semiconductor (ε_S = 3.9),[22] ε_0 is the permittivity of vacuum, T is the absolute temperature, T_0 is a parameter that indicates the width of the exponential distribution, σ_0 is the pre-factor of the conductivity, α^{-1} is the effective overlap parameter between localized states, B_C is a critical number for the onset of percolation, V_{SO} is the switch-on voltage, V_G and V_D are the gate and drain voltage, respectively, and C_i is the insulator capacitance per unit area. Figure 2b shows the experimental transfer characteristics (symbols) obtained at T = 293 K and T = 192 K, with the corresponding fits (solid lines). For B_C, a value of 2.8 was used.[28] Fitting was performed using a single set of values for the three parameters T_0, σ_0, and α^{-1}, namely

$T_0 = 400$ K, $\sigma_0 = 8 \times 10^7$ S m^{-1}, and $\alpha^{-1} = 0.105$ nm. It is evident in Figure 2b that for $T = 293$ K and $V_G < +30$ V, the experimental data cannot be accurately described by Equation 1. This is not the case, however, for $T = 192$ K, where the fittings are in good agreement with the experimental data throughout the measurement range. This discrepancy is attributed to a high contact resistance at the Au/PCBM interface, which dominates current flow through the device at low gate voltages. In the case of PCBM sandwich diodes, it was demonstrated that the use of Au contacts leads to strong injection-limited current characteristics. However, when Au was replaced by ohmic contacts, such as LiF/Al, the current was found to increase by more than two orders of magnitude.[23] Moreover, earlier reported experiments have shown that the contact resistance (R_C) can easily dominate the effective channel resistance (R_{CH}) in pentacene-based OFETs.[29] To investigate this in more detail, we measured the output characteristics of the transistor at 293 K (Fig. 3a). It can be seen that for high V_G, the transistor operates in electron-enhancement mode and its performance is similar to a unipolar n-type transistor. However, close examination of this figure at $V_D < +2$ V reveals nonlinear current characteristics, indicating the existence of an injection barrier which will contribute to R_C. To determine how R_C compares with R_{CH}, we calculated both by plotting the total device resistance (R_{ON}) in the linear regime ($V_D \ll V_G$), given as $R_{ON} \equiv \partial I_D / \partial V_D$ (where $R_{ON} = R_C + R_{CH}$) against the channel length.[30,31] From the intercept of the extrapolated characteristic at $L = 0$ μm with the y-axis, the value for R_C can be calculated, whereas from the slope of the characteristic the R_{CH} per unit channel length is obtained. Figure 3b shows the ratio of R_C/R_{CH} as a function of V_G measured at two different temperatures. Note that the error bars are significant due to the uncertainty in the slope and intercept parameters obtained from the R_{ON} versus L plots, and are dominated by device-to-device fluctuations. Additional errors may also arise from calculation of R_C in short-channel devices where the influence of higher electric fields (as compared to long L devices) is not taken into account. Nevertheless, for all samples the general trend of decreasing R_C/R_{CH} with increasing V_G is observed.

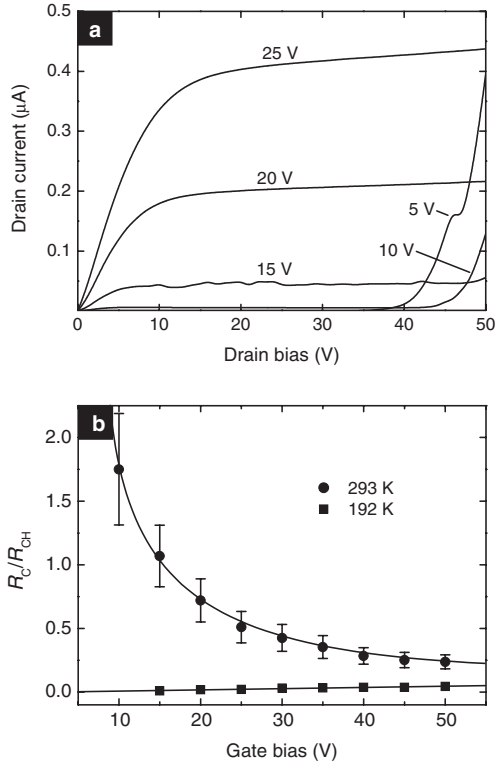

Figure 3. a) Output characteristics of a PCBM field-effect transistor ($L = 20$ μm) operating in electron-accumulation mode at different gate voltages. b) Ratio of the contact resistance over channel resistance (R_C/R_{CH}) as a function of gate voltage (V_G) for an $L = 20$ μm FET measured at 192 K (■) and 293 K (●). The lines are to guide the eye.

It is evident from the high temperature (293 K) characteristic in Figure 3b that, for low gate biases, the contact resistance is larger than the channel resistance. Consequently, Equation 1 is no longer valid simply because it is based on the assumption of ohmic contacts. Only for $V_G > +30$ V does the R_C/R_{CH} ratio become considerably small, so Equation 1 can be used to accurately describe the measured transfer characteristics. Now, the question that arises is why the model describes the transfer characteristics at low temperatures better. This can be explained by considering the temperature dependence of $R_{CH} = L/W\mu(T)\,|V_D|\,C_i$. As the temperature drops, the mobility, described by $\mu \propto \exp(-E_\mu/k_B T)$, decreases, and therefore R_{CH} increases and eventually dominates the conduction across the device. However, one could argue that R_C is also temperature dependent and increases with decreasing temperature too ($R_C \propto \exp[E_C/kT]$).[32] The answer to this argument comes from the findings of Woudenbergh et al.,[33] who showed that the thermal activation (E_C) of injection-limited currents in polymer/metal contacts is weaker than the thermal activation of the mobility (E_μ). In the latter work, experimental results were interpreted in terms of thermally assisted hopping of charges from the electrode into the localized states of the polymer, which are broadened due to disorder.[33] Similarly, Bürgi et al.[32] have reported that the temperature dependence of the contact resistance in poly(3-hexylthiophene)- and poly(9,9′-dioctylfluorene-*co*-bithiophene)-based transistors with contact-potential barriers $\phi_b \geq 0.3$ eV is much weaker than that of the channel resistance. For the present work, this effect is clearly demonstrated in Figure 3b, where the ratio of R_C/R_{CH}, measured at 192 K, exhibits a rather small gate-voltage dependence, with R_C being significantly smaller than R_{CH} throughout the measured V_G range. Hence, relative to the channel resistance at low temperatures, R_C becomes less significant for the total device resistance, supporting the idea that transport is a bulk-limited rather than a contact-limited process. Similar findings have also been reported for polymeric FETs employing similar device architectures.[34] However, quantitative analysis of the effect of R_C on the conduction mechanism across the PCBM transistors will require further experimental investigations, which is beyond the scope of this work.

ADVANCED MATERIALS

We will now consider operation of the PCBM transistors in hole-accumulation mode. Examination of Figure 3a reveals an increase in I_D for $V_D > +40$ V at $V_G = +5$ and +10 V. This observation is very significant, since it resembles the characteristic of an ambipolar transistor and has not been reported previously, neither for PCBM nor for C_{60} FETs. This large increase in I_D is a result of a hole-accumulation region induced near the drain contact when $V_D > V_G + V_{SO(p)}$, where $V_{SO(p)}$ is the switch-on voltage for the p-channel mode of operation. To investigate this further, we measured the room-temperature transfer characteristics of a typical PCBM-based FET ($L = 20$ μm) in hole-accumulation mode (Fig. 4a). For this purpose, the gate and drain electrodes are biased negatively with respect to the grounded source electrode. It is found that the transfer curves exhibit typical p-channel behavior with the

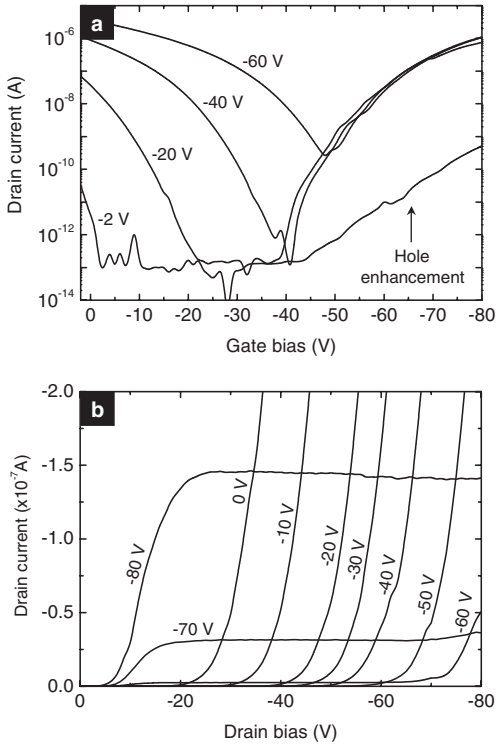

Figure 4. Room-temperature transfer and output characteristics of a typical PCBM field-effect transistor ($L = 20$ μm) in p-channel operation. a) Transfer characteristics at different drain voltages, and b) output characteristics at different gate voltages.

creation of a hole-enhancement current under appropriate bias conditions ($|V_G| > |V_D|$). The hole-drain current increases significantly as the gate electrode is biased even more negatively, and reaches a value of $\approx 10^{-6}$ A for $V_G = -80$ V. In all measurements, the drain currents are more than a factor of ten higher than the corresponding measured gate currents, emphasizing the real p-channel operation of the PCBM-based transistors. The large switch-on voltage of –30 V to –40 V suggests either a significant density of hole traps at the SiO_2/PCBM interface, or that the current level in the linear regime is lower than our instrument's detection limit for $0 < |V_G| < 20$ V. The low hole current is presumably due to the presence of the large injection barrier for holes ~1.64 eV, if one includes contributions from interface dipoles. The field-effect mobility for holes (μ_h) in the saturation regime is 8×10^{-3} cm^2 V^{-1} s^{-1}, at $V_G = -75$ V, with the ON–OFF current ratio on the order of 10^6. Consequently, these measurements demonstrate for the first time that the mobilities of electrons and holes in a fullerene-based transistor are approximately equal. Values for the field-effect hole mobility in the linear regime could not be reliably calculated since the contact resistance (see Fig. 4b), induced by interface effects, dominates conduction across the device. Figure 4b shows the output characteristics of the PCBM transistor in p-channel operation. For $V_G = -70$ and –80 V, a characteristic p-channel transistor operation is observed. Although this is also the case for the output characteristics for $V_G = -40$ to –60 V, this feature is not clearly visible due to the scale of Figure 4b. For gate biases in the range –50 to –70 V, the output characteristics exhibit an increase in the drain current for $|V_D| > |V_G| + |V_{SO(n)}|$, where $V_{SO(n)}$ is the switch-on voltage for the n-channel. Under this particular set of bias conditions, electrons are injected from the drain contact, and therefore contribute to the total current flowing through the device. The nonlinear output characteristics observed at low V_D biases (see, for example, characteristics for $V_G = -70$ V and –80 V) are consistent with the presence of a large injection barrier for holes $\phi_b(h^+) = 1.64$ eV discussed earlier. To the best of our knowledge, this is the first example of ambipolar charge transport in a FET based on neat PCBM, and can be viewed as a significant step forward in the development of organic complementary-like circuits.

In conclusion, ambipolar charge transport in solution-processed PCBM-based OFETs has been demonstrated even though high-work-function gold electrodes are employed. Under appropriate biasing conditions, the transistors exhibit electron and hole mobility on the order of 1×10^{-2} cm^2 V^{-1} s^{-1} and 8×10^{-3} cm^2 V^{-1} s^{-1}, respectively. The ON–OFF current ratio is on the order of 10^6 for both n- and p-channel operation. The present results qualify PCBM as a potential candidate for application in organic complementary-like technology based on a single solution-processible semiconductor. In addition, they provide further experimental evidence for the ambipolar character of pure organic semiconductors.

Experimental

Field-effect transistors were made using heavily doped p-type Si wafers as gate electrodes with a 200 nm-thick thermally oxidized SiO_2 layer as the gate dielectric. Using conventional photolithography, gold source and drain electrodes were defined with channel widths of 1000 μm and lengths in the range of 0.75–40 μm. A 10 nm thick layer of titanium was used as an adhesion layer for the gold on the SiO_2. The SiO_2 layer was treated with the primer hexamethyldisilazane prior to semiconductor deposition in order to make the surface hydro-

phobic. The drain electrode was contained within a circular source electrode in order to minimize parasitic leakage currents [21]. Films were spun from a 10 mg mL^{-1} solution of [6,6]-phenyl-C_{61}-butyric acid methyl ester (PCBM) in chlorobenzene at 500 rpm for 1 min. Prior to spin-coating, the solution was stirred for one hour at 80 °C and then filtered using Millipore Millex-FH 0.45 μm poly(tetrafluoroethylene) filters. All freshly fabricated devices were annealed in vacuum of 10^{-5} Pa at 120 °C for several hours. All electrical measurements were performed at room temperature (20 °C) using an HP 4156B semiconductor parameter analyzer in a high vacuum of 10^{-5} Pa due to the instability of the devices under ambient conditions. It was found that PCBM exhibits poor wetting behavior on the substrate used, resulting in slightly non-uniform films. Upon annealing for several hours, PCBM films appear microcrystalline and rough.

Received: March 3, 2004
Final version: July 21, 2004

[1] R. H. Friend, R. W. Gymer, A. B. Holmes, J. H. Burroughes, R. N. Marks, C. Taliani, D. D. C. Bradley, D. A. Dos Santos, J. L. Bredas, M. Lögdlund, W. R. Salaneck, *Nature* **1999**, *397*, 121.
[2] A. J. Heeger, *Angew. Chem. Int. Ed.* **2001**, *40*, 2591.
[3] C. D. Dimitrakopoulos, P. R. L. Malenfant, *Adv. Mater.* **2002**, *14*, 99.
[4] P. Peumans, A. Yakimov, S. R. Forrest, *J. Appl. Phys.* **2003**, *93*, 3693.
[5] Z. Liu, A. A. Yasseri, J. S. Lindsey, D. F. Bocian, *Science* **2003**, *302*, 1543.
[6] C. J. Drury, C. M. Mutsaers, C. M. Hart, M. Matters, D. M. de Leeuw, *Appl. Phys. Lett.* **1998**, *73*, 108.
[7] G. H. Gelinck, H. E. A. Huitema, E. van Veenendaal, E. Cantatore, L. Schrijnemakers, J. B. P. H. van der Putten, T. C. T. Geuns, M. Beenhakkers, J. B. Giesbers, B.-H. Huisman, E. J. Meijer, E. M. Benito, F. J. Touwslager, A. W. Marsman, B. J. E. van Rens, D. M. de Leeuw, *Nat. Mater.* **2004**, *3*, 106.
[8] A. R. Brown, C. P. Jarrett, D. M. de Leeuw, M. Matters, *Synth. Met.* **1997**, *88*, 37.
[9] H. Sirringhaus, N. Tessler, R. H. Friend, *Science* **1998**, *280*, 1741.
[10] C. D. Dimitrakopoulos, S. Purushothaman, J. Kymissis, A. Callegari, J. M. Shaw, *Science* **1999**, *283*, 822.
[11] R. C. Haddon, A. S. Perel, R. C. Morris, T. T. M. Palstra, A. F. Hebard, R. M. Fleming, *Appl. Phys. Lett.* **1995**, *67*, 121.
[12] J. G. Laquindanum, H. E. Katz, A. Dodabalapur, A. J. Lovinger, *J. Am. Chem. Soc.* **1996**, *118*, 11 331.
[13] H. E. Katz, A. J. Lovinger, J. Johnson, C. Kloc, T. Siegrist, W. Li, Y.-Y. Lin, A. Dodabalapur, *Nature* **2000**, *404*, 478.
[14] M. Matsumura, Y. Nara, *J. Appl. Phys.* **1980**, *51*, 6443.
[15] A. Dodabalapur, H. E. Katz, L. Torsi, R. C. Haddon, *Science* **1995**, *269*, 1560.
[16] A. Dodabalapur, H. E. Katz, L. Torsi, R. C. Haddon, *Appl. Phys. Lett.* **1996**, *68*, 1108.
[17] K. Tada, H. Harada, K. Yoshino, *Jpn. J. Appl. Phys., Part 2* **1996**, *35*, L944.
[18] a) R. Martel, V. Derycke, C. Lavoie, J. Appenzeller, K. K. Chan, J. Tersoff, Ph. Avouris, *Phys. Rev. Lett.* **2001**, *87*, 256 805. b) J. A. Misewich, R. Martel, Ph. Avouris, J. C. Tsang, S. Heinze, J. Tersoff, *Science* **2003**, *300*, 783.
[19] E. J. Meijer, D. M. de Leeuw, S. Setayesh, E. van Veenendaal, B.-H. Huisman, P. W. M. Blom, J. C. Hummelen, U. Scherf, T. M. Klapwijk, *Nat. Mater.* **2003**, *2*, 678.
[20] R. J. Chesterfield, C. R. Newman, T. M. Pappenfus, P. C. Ewbank, M. H. Haukaas, K. R. Mann, L. L. Miller, C. D. Frisbie, *Adv. Mater.* **2003**, *15*, 1278.
[21] E. J. Meijer, C. Detcheverry, P. J. Baesjou, E. van Veenendaal, D. M. de Leeuw, T. M. Klapwijk, *J. Appl. Phys.* **2003**, *93*, 4831.
[22] V. D. Mihailetchi, J. K. J. van Duren, P. W. M. Blom, J. C. Hummelen, R. A. J. Janssen, J. M. Kroon, M. T. Rispens, W. J. H. Verhees, M. M. Wienk, *Adv. Funct. Mater.* **2003**, *13*, 43.
[23] J. K. J. van Duren, V. D. Mihailetchi, P. W. M. Blom, T. van Woudenbergh, J. C. Hummelen, M. T. Rispens, R. A. J. Janssen, M. M. Wienk, *J. Appl. Phys.* **2003**, *94*, 4477.
[24] S. C. Veenstra, A. Heeres, G. Hadziioannou, G. A. Sawatzky, H. T. Jonkman, *Appl. Phys. A: Solids Surf.* **2002**, *75*, 661.
[25] C. Waldauf, P. Schilinsky, M. Perisutti, J. Hauch, C. J. Brabec, *Adv. Mater.* **2003**, *15*, 2084.
[26] C. Tanase, E. J. Meijer, P. W. M. Blom, D. M. de Leeuw, *Phys. Rev. Lett.* **2003**, *91*, 216 601.
[27] a) M. C. J. M. Vissenberg, M. Matters, *Phys. Rev. B: Condens. Matter Mater. Phys.* **1998**, *57*, 12 964. b) E. J. Meijer, C. Tanase, P. W. M. Blom, E. van Veenendaal, B.-H. Huisman, D. M. de Leeuw, T. M. Klapwijk, *Appl. Phys. Lett.* **2002**, *80*, 3838.
[28] G. E. Pike, C. H. Seager, *Phys. Rev. B: Solid State* **1974**, *10*, 1421.
[29] a) H. Klauk, G. Schmid, W. Radlik, W. Weber, L. Zhou, C. D. Sheraw, J. A. Nichols, T. N. Jackson, *Solid-State Electron.* **2003**, *47*, 297. b) P. V. Necliudov, M. S. Shur, D. J. Gundlach, T. N. Jackson, *Solid-State Electron.* **2003**, *47*, 259.
[30] H. Sirringhaus, N. Tessler, D. S. Thomas, P. J. Brown, R. H. Friend, *Adv. Solid State Phys.* **1999**, *39*, 101.
[31] E. J. Meijer, G. H. Gelinck, E. Van Veenendaal, B.-H. Huisman, D. M. de Leeuw, T. M. Klapwijk, *Appl. Phys. Lett.* **2003**, *82*, 4576.
[32] L. Bürgi, T. J. Richards, R. H. Friend, H. Sirringhaus, *J. Appl. Phys.* **2003**, *94*, 6129.
[33] T. van Woudenbergh, P. W. M. Blom, M. C. J. M. Vissenberg, J. N. Huiberts, *Appl. Phys. Lett.* **2001**, *79*, 1697.
[34] a) B. H. Hamadani, D. Natelson, *Appl. Phys. Lett.* **2004**, *84*, 443. b) B. H. Hamadani, D. Natelson, *J. Appl. Phys.* **2004**, *95*, 1227.

Linear Assemblies of Silica-Coated Gold Nanoparticles Using Carbon Nanotubes as Templates**

By *Miguel A. Correa-Duarte*,* *Neli Sobal*, *Luis M. Liz-Marzán*, and *Michael Giersig**

The fabrication of nanostructures and nanoarrays based on metal nanoparticles is a major topic in nanotechnology because of their potential applications in fields such as electronics,[1] photonics,[2] and catalysis.[3] Noble-metal nanoparticles display very interesting optical properties, which arise from the coupling of incoming light with the collective oscillation of conduction electrons (surface plasmons).[4] It has been shown that the precise position of the surface-plasmon band depends on parameters such as particle size and shape,[5] but also on the nature of the surrounding medium[6] and on the

[*] Dr. M. A. Correa-Duarte, Dr. M. Giersig, Dr. N. Sobal
Center of Advanced European Studies and Research (CAESAR)
Ludwig-Erhard-Allee 2, D-53175 Bonn (Germany)
E-mail: macorrea@uvigo.es; giersig@caesar.de
Prof. L. M. Liz-Marzán
Departamento de Química Física
Universidade de Vigo, E-36310, Vigo (Spain)

[**] Prof. K. Kempa and Prof. Z. Ren from Boston College and Nanolab Inc. are acknowledged for supplying both powdered and aligned MWNT samples.

 DOI: 10.1002/adma.200400626